



Studies of surface interactions at nanometer scale with atomic force microscopy combined with scanning electron microscopy
by Huddee J Ho

A thesis submitted in partial fulfillment of the requirements for the degree of Doctor of Philosophy in Physics
Montana State University
© Copyright by Huddee J Ho (1997)

Abstract:

The Atomic Force Microscope (AFM) is an important instrument measuring surface topography and related phenomena; and can study nanometer-scale surface interactions. Surface interactions in ambient air are complicated by surface contamination layers, which do not occur in vacuum or liquid environments. This thesis studies nanometer scale surface interactions, in ambient air, using AFM's high force sensing capability. Several experimental methods were developed and new insights into surface interactions at nanometer scale were obtained. Substantial improvement was made on the lateral resolution of AFM operation in air.

To position the force sensing tip over a specific nanometer scale area, a novel instrument combining AFM and Scanning Electron Microscopy (SEM) was designed, built and commissioned. The system is capable of analyzing AFM tip conditions, in order to study the effects of tip/surface contact. An essentially new method, which monitors the dynamic sensor signal and its fluctuation while changing the tip-sample gap, was developed for vibrating cantilever studies. Sometimes, an electrostatic force occurs in surface contamination, which can be measured with scanning Kelvin probe force microscopy (KFM); this made it possible to develop a technique for probing surface contamination electrical properties.

A capillary force is associated with the contamination layer. Both capillary force magnitude and layer thickness were measured by fitting the approach curve with the capillary force theoretical model. Studying capillary force with cantilevers of differing spring constants, we demonstrated that capillary force can be balanced by a cantilever having a sufficiently large spring constant. With KFM, the contamination layer was found to contain a charge distribution that changes with time. A model is proposed, showing that the surface contamination layer contains a molecular layer bonded tightly to the sample surface. With KFM, dopant concentration was measured on an MBE-grown semiinsulating sample cross-section, and electrical potential scan edge effect was observed. Systematically studying tip-sample contact, two types of contact processes were identified: jump-to-contact and ramp-to-contact, and the conditions under which they occur. A new spatial region (near-contact region), minimizing tip-sample gap without tip-sample contact, was discovered. Operating in the near-contact region is the optimal operating mode of a vibrating cantilever AFM.

STUDIES OF SURFACE INTERACTIONS AT NANOMETER SCALE WITH
ATOMIC FORCE MICROSCOPY COMBINED WITH
SCANNING ELECTRON MICROSCOPY

by

Huddee J Ho

A thesis submitted in partial fulfillment of the
requirements for the degree

of

Doctor of Philosophy

in

Physics

MONTANA STATE UNIVERSITY
Bozeman, Montana

April 1997

D378
H65

APPROVAL

of a thesis submitted by

Huddee J Ho

This thesis has been read by each member of the thesis committee and has been found to be satisfactory regarding content, English usage, format, citations, bibliographic style, and consistency, and is ready for submission to the College of Graduate Studies.

April 15, '97
Date

Lerald J. Lapeyre
Chairperson, Graduate Committee

Approval for the Major Department

4-15-97
Date

[Signature]
Head, Major Department

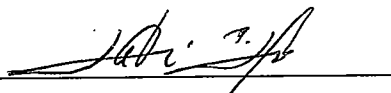
Approval for the College of Graduate Studies

4/16/97
Date

[Signature]
Graduate Dean

STATEMENT OF PERMISSION TO USE

In presenting this thesis in partial fulfillment of the requirements for a doctoral degree at Montana State University-Bozeman, I agree that the library shall make it available to borrowers under rules of the Liberty. I further agree that copying of this thesis is allowable only for scholarly purposes, consistent with "fair use" as prescribed in the U. S. Copyright Law. Requests for extensive copying or reproduction of this thesis should be referred to University Microfilms International, 300 North Zeeb Road, Ann Arbor, Michigan 48106, to whom I have granted "the exclusive right to reproduce and distribute my dissertation in and from microform along with the non-exclusive right to reproduce and distribute my abstract in any format in whole or in part."

Signature 
Date April 14, 1997

To my daughter, Rebecca

ACKNOWLEDGMENTS

This has been the most difficult project of my life. I would like to thank Professor Gerald Jerry Lapeyre whose continued support made this thesis possible.

The research of this thesis was performed at TopoMetrix Corporation's Santa Clara facility, where I received assistance from almost everyone. My greatest thanks to Dr. Paul West. He initiated the idea of doing my Ph.D. thesis in the industry environment, and continuously encouraged me to finish this thesis over the past few years. I am also indebted to other staff at TopoMetrix: Mr. Marc Schuman, who provided electronics support; Ms. Joni Li, whose software tools made my PPM data analysis easy; Dr. Kong Loh, who shared his expertise on loading curves and with whom I had some stimulating discussions on the near-contact mode; and the technical writing experts, Mr. Tony Marek, Mr. Stephen Eichelberger, and Mr. Rick Castagner who helped me on grammar and writing style.

I am also grateful to Dr. James Anderson, who gave me UHV lab training while I was working in the CRISS lab, and contributed many hours of his time in reviewing this dissertation. I would like to thank Professor Jingde Li of Zhongshan University, who taught me all the fundamental skills of building scientific instruments. My four-and-a-half years of research experience on ferroelectric ceramics under his supervision has been extremely helpful for me in designing various PPMs. Thanks are also due to Michael T. Postek of the National Institute of Standards and Technology and Mrs. Nancy Lapeyre for reviewing the thesis and giving a lot of great comments.

I would like to thank my family, for understanding my long work hours. I am deeply indebted to my daughter, Rebecca, who taught me the meaning of life.

TABLE OF CONTENTS

APPROVAL	ii
STATEMENT OF PERMISSION TO USE	iii
ACKNOWLEDGMENTS	v
TABLE OF CONTENTS	vi
LIST OF TABLES	x
LIST OF FIGURES	xi
ABSTRACT	xvii
ACRONYMS	xviii
1. INTRODUCTION	1
2. HISTORICAL REVIEW	7
Introduction	7
Nanometer Scale Force Sensing Techniques	11
Cantilever-Based Force Sensors	12
Tunneling Sensor	15
Capacitance Sensor	15
Interferometer Sensor	15
Optical Deflection Sensor	16
Piezoresist Sensor	16
Shear Force Sensors	17
Impedance Sensor	17
Quartz Tuning Fork Sensor	18
Ranging Techniques for Locating Nanometer Scale Objects	18
Combining STM/AFM and SEM	20
Vibrating Cantilever Mode of AFM Operation	21
Nanometer Scale Surface Electrical Potential Sensors	24
Kelvin-probe Force Microscopy	25
Maxwell Stress Microscopy	27
3. THEORETICAL ANALYSIS	29
Introduction	29
Nanometer Scale Surface Interactions	29

Interaction between Neutral Molecules	30
Interaction between a Sphere and a Flat Surface	33
van der Waals Force	33
Capillary Force	33
Comparing van der Waals Force with Capillary Force	35
Lateral Resolution in Imaging the Electrostatic Properties	36
Mechanical Resonance of a Harmonic Oscillator with Viscous Damping	41
Tip-Sample Contact: Harmonic Oscillator with Non-Damping Force	43
Surface Electrical Potential on Semiconductors	52
Summary	56
4. EXPERIMENTAL APPARATUS	57
Introduction	57
Design of the Combined PPM/SEM System	57
Design Objectives of the Instrument	58
Overview of the Instrument	60
PPM Head	63
Piezoelectric Scanners	65
Sample and Probe Replacement	66
Vibration Isolation System	66
Translation Stages	68
Control System	69
Direct Probe Viewing	69
Testing the Performance of the PPM/SEM System	71
Operation in Vacuum	71
Simultaneous PPM/SEM Operation	73
Aging of Piezoelectric Scanner	74
Vibration Isolation and Atomic Resolution	76
Studies of Tip Conditions	79
Locating Sub-micrometer Features	79
Vibrating Cantilever Mode AFM System	82
System Structure	82
Amplitude Detection Mode	86
Phase Detection Mode	86
System Performance	87
Operation in Vacuum	88
Double-Feedback-Loop Surface Potential Sensing System	92
Potential measurement	92
Spatial Resolution	96
Operation Parameters	99
AFM Probes	99
Silicon Nitride Probe	99
Silicon Probe	100
VLS Silicon Probe	100
Summary	102
5. STUDIES OF AFM LOADING CURVES	103

Introduction	103
Experiments	104
Measuring Force with a Micro Cantilever	104
Measuring a Loading Curve	106
Calibrating a Loading Curve	108
Interpreting a Loading Curve	111
Comparing Loading Curves in Air and in Vacuum	112
Results and Analysis	113
Reproducibility of the Measurements	113
Loading Curves for Cantilevers of Different Spring Constants	117
Surface Contamination Studies	120
Conclusion	125
6. STUDIES OF VIBRATING CANTILEVER MODE	126
Introduction	126
Experiments	128
Experiment One: Changes in Tip Geometry by Periodic Contact	128
Experiment Two: Wear of a Silicon Tip on a Silicon Sample	135
Experiment Three: Surface Modification by Periodic Contact	135
Experiment Four: Monitoring the Tip Approach Process	140
Experiment Five: Comparison of Three Distinct Operation Modes	143
Experiment Six: Estimating Lateral Resolution	149
Results and Analysis	153
Optimal Parameters of VCM Operation	153
Effect of the Spring Constant of Cantilevers	153
Effect of the Driving Frequency	155
Effect of the Vibration Amplitude	157
Amplitude Detection versus Phase Detection	157
Effect of the Phase Setting	157
Working Principle of the VCM Operation	158
Concepts of Contact and Non-Contact	158
Theoretical Model of Tip-Contamination-Sample System	159
Mechanism of Feedback Establishment	164
Mechanism of Tip Damage	165
Classification of the Three Different VCM Operation Modes	168
Examples of Ultra-high Resolution AFM Imaging in Near-Contact Mode	172
Metal Film Samples	172
Semiconductor Samples	172
Insulating Samples	175
Soft Polymer Samples	175
Biological Samples	175
Conclusion	180
7. IMAGING SURFACE ELECTRICAL POTENTIAL	183
Introduction	183
Scanning Kelvin-probe Force Microscopy	183
Imaging the Surface of a PZT Film	186

Designing and Studying a Standard Sample	189
Studies of Sub-Micrometer MBE Grown Layers	197
Sample Preparation	198
Locating the Area of MBE Layer	200
Surface Potential Imaging	200
Results and Analysis	203
Conclusion	205
8. CONCLUSIONS	207
Proximal Probe Microscopy	207
Experimental Apparatus and Methods	208
Surface Contamination and Capillary Force	209
Optimal Operation Conditions for the Vibrating Cantilever Mode AFM	210
Nanometer Scale Surface Potential Measurement	211
Future Studies	212
REFERENCES CITED	213

LIST OF TABLES

Table	Page
1. Parameters of the three silicon cantilevers used for the loading curve comparison.....	118
2. Experimental parameters of the three different VC operation modes.....	143
3. Comparison of energy dissipation.....	168
4. Characteristics of the three VCM operation.....	171

LIST OF FIGURES

Figure	Page
2.1. The operation of a PPM. (a) Initial set-up; (b) The tip approach process; (c) The scanning process.....	9
2.2. Cantilever-based force sensor.....	13
2.3. Shear force sensor.....	14
2.4. The working principle of the AFM vibrating cantilever mode (VCM).....	22
3.1. The force created by the Lennard-Jones Potential.....	32
3.2. The capillary attraction between a sphere and a flat surface.....	34
3.3. Comparison of the van der Waals force and capillary force between a sphere and a flat surface for two different values of the radius, R	35
3.4. Diagram of a single charge and a conducting sphere.	36
3.5. Definition of the lateral resolution.	38
3.6. Electrostatic force between a single charge and a conducting tip.....	40
3.7. The resonance spectra of a driven damped harmonic oscillator.	42
3.8. Jump-to-contact and ramp-to-contact.	44
3.9. A simplified model of a vibrating probe in an attractive interaction with the sample. The interaction force has a positive gradient.....	46
3.10. The total force applied to the AFM probe and the conditions of JTC: (a) JTC occurs when $x < x_J$; (b) JTC never occurs; (c) JTC always occurs; (d) JTC occurs only for $x_J = 0$	48
3.11. Conditions of JTC as a function of the relative tip-sample gap μ and the relative spring constant λ	49
3.12. Simple Harmonic Oscillator under an attractive force between the tip and the sample. In this example, $x_0 = 50$ nm, $x_1 = 10$ nm.	51

3.13. Energy loss when the tip encounters a rigid surface in RTC.....	53
3.14. (a) Diagram of a sharp p-n junction; ⁵⁵ (b) Dopant concentration and net charge density; (c) Electrical potential.....	55
4.1. Configuration diagram of the PPM/SEM combination.....	59
4.2. Diagram of the PPM integrated with a scanning electron microscope.....	61
4.3. Picture of the PPM unit removed from the SEM specimen chamber.....	62
4.4. Diagram of the PPM head. (A) laser diode, (B) primary deflection mirror, (C) secondary mirror, (D) photoelectric sensor, (E) Sample, (F) piezo tube, (G) AFM scanner, (H) STM scanner, (I) primary XY translator, (J) manual adjustment screw, (K) motorized screw, (L) DC motor.....	64
4.5. The vibration isolation system.....	67
4.6. Schematic diagram of the electronic control system.....	70
4.7. Examples of different tip conditions of a type of commercially available silicon AFM tip. (a) A tip that was not etched completely. (b) A regular sharp tip.....	72
4.8. Images of highly-oriented-poly-graphite (HOPG) acquired in the SEM. (a) AFM force image. The field of view is 30 Å. (b) STM tunneling current image. The field of view is 12 Å. The bias voltage was 50 mV. The tunneling current was 1 nA.....	77
4.9. The background noise spectra of the feedback signals.....	78
4.10. SEM micrograph of a VLS silicon AFM tip before (a) and after (b) usage. The image on the right side is the enlarged tip area of the left image. The increase of the magnification is ten times. The scale bar on the bottom is for the image on the left side. For the right image, each division represents 66.7 nm.....	80
4.11. Near-contact AFM image of an aluminum grain sample. There are two deep scratch marks and one shallow scratch mark in the image area. The image size is 1.6 mm × 1.6 mm. The image was acquired in air. The cantilever vibration amplitude was 2 nm.....	81
4.12. Studies of micro crack in ceramic. (a-c) SEM images; (d) an AFM image. The size of the AFM topographic image is 2 × 2 μm.....	83

4.13. Diagram of the electronics for operating the vibrating cantilever mode AFM.....	84
4.14. Selecting the operation frequency.....	85
4.15. Transfer function of the control electronics in amplitude mode.....	89
4.16. Frequency spectrum of amplitude and phase signals.....	90
4.17. Selecting the drive frequency for vacuum operation.....	91
4.18. Vibrating cantilever AFM images acquired in two environments: (a) in air; (b) in vacuum. The sample is an aluminum film on silicon substrate.....	93
4.19. Diagram of the double-feedback loop surface potential sensing system.....	94
4.20. Wiring diagram of the surface potential imaging system.....	95
4.21. Testing the potential measurement.....	97
4.22. Spatial resolution of KFM.....	98
4.23. The AFM probes used in this dissertation. (a) Silicon nitride with FIB sharpening; (b) Single-crystal silicon probe; (c) Silicon tip grown with the VLS technique.....	101
5.1. Diagram of the cantilever bending.....	105
5.2. Mechanism of force detection with the optical deflection force sensing system.....	106
5.3. An experimental loading curve.....	107
5.4. An example of loading-curve calibration using an approach curve measured in air: (a) As measured. (b) Cantilever-deflection corrected from the measured curve in (a).....	110
5.5. Jump-to-contact and adhesive pullback.....	112
5.6. Repeatable loading curves measured consecutively.....	114
5.7. Loading curves measured on different samples.....	115
5.8. Loading curves for cantilevers of different spring constant.....	119
5.9. Comparison of the approach curves in the loading curves of three cantilevers with different spring constants near the tip-surface contact point.....	121
5.10. The loading curves measured in air and in vacuum with the same cantilever on the same sample area.....	123
5.11. Fitting the approach curve with a simplified model of capillary attraction force. $R = 800$ nm, $G_0 = 11.6$ nm.....	124

6.1. The resonance spectrum of the VLS silicon probe.....	129
6.2 SEM image of the VLS silicon tip. (a) Before any topographic AFM image was acquired, (b) after three hours of imaging with a small (8 nm) vibration amplitude with a 40% reduction in amplitude, and (c) after one topographic image with 80 nm vibration with a 10% reduction in amplitude. The scale dots on the lower right corner is for the image in the left. The right image corresponds to the box in the left image. Its scale is 1/10 of the left image.....	131
6.3. Topographic images (shaded view) of aluminum grains: (a) with 8 nm vibration amplitude and (b) with 80 nm vibration amplitude. The size of both images is 800×800 nm.	132
6.4. Spatial frequency spectrum of the topographic images illustrated in Figure 6.3.	134
6.5. SEM image of a silicon tip before imaging a silicon surface (a) and after imaging with an vibration amplitude of 100 nm and a 10% reduction in amplitude (b).....	136
6.6. The mechanism of sample damage.....	138
6.7. The near-contact AFM images (a)-(c) show that the sample is damaged by periodic contact operation.	139
6.8. The SEM micrographs taken before and after the experiment (shown in Figure 6.7) show no obvious change in the tip profile.....	141
6.9. The transition from traditional non-contact to near-contact.	142
6.10. Resonance spectrum of the silicon tip (Model 1650-00 #25).....	144
6.11. Topographic images of a polished alumina-silicate glass surface with three distinct operation modes. (a) Near-contact mode; (b) Traditional non-contact mode; (c) Periodic contact mode. The image size is 100 nm × 100 nm.	145
6.12. Line profiles of the same features in the three VC modes.	147
6.13. Spatial frequency spectrum of the three VC mode operation conditions.	148
6.14. SEM images of the tip before and after acquiring the three VC mode AFM images.	150

6.15. Topographic image of a niobium film sample that has the potential of being a standard sample for tip geometry characterization. (a) The image is displayed with pseudo-2D color (90/140); (b) the area of the box in (a), displayed in 1D color.....	151
6.16. A set of consecutive line profiles from a zoomed section of the image (Figure 6.15(b)). The scan lines are displayed by shifting 1 nm upward from the previous scan line.	152
6.17. Relationship between the drive frequency and the feedback setpoint.....	156
6.18. Microscopic model of tip-contamination-sample system.....	161
6.19. Molecular model of tip approaching process in ambient air.....	163
6.20. Diagrams of the mechanism of the three VC mode operation conditions: (a) traditional non-contact condition; (b) periodic contact condition; (c) near-contact condition.....	166
6.21. Classification of three VC modes by the three different stages of tip-sample interaction.....	170
6.22. Aluminum film on a silicon wafer.....	173
6.23. Atomically flat cleavage surface of GaAs.....	174
6.24. Polished alumina-silicate glass substrate.....	176
6.25. Epoxy acrylic coating.....	177
6.26. Two types of soft polymer thin-film samples.....	178
6.27. Human infant hair sample.....	179
7.1. Separating the surface electrostatic information from the topographic information. (a) There is only the non-contact topographic feedback loop. The sample has no surface potential change. (b) There is localized surface charge on the sample. (c) Topographic feedback plus the potential feedback for the sample with localized surface charge.....	185
7.2. Images of a PZT ceramic surface: (a) before, (b and c) after the surface potential feedback loop is turned on.....	187
7.3. Comparison of topography line profiles before and after the surface potential feedback loop is turned on.....	188
7.4. Time dependence studies of KFM on a PZT ceramic surface.....	190

7.5. Design of the standard sample for electrical potential measurement.	191
7.6. Simultaneous topographic (a) and surface potential (b) images of the standard sample. The electrodes labeled "A" were always connected to ground. The electrodes labeled "B" were connected to a voltage source controlled by the software. Each image has 300 scan lines. Each line has 300 data points.	192
7.7. Line No. 80 of the images showed in Figure 7.6.	194
7.8. Three line profiles from the potential image show the relative of the potential changes.	195
7.9. The GaAs MBE grown multilayer sample.	198
7.10. The surface topography of cleavage surfaces. (a) a bad cleave. (b) a good cleave.	199
7.11. SEM view showing positioning of the AFM tip over the area of MBE layers.	201
7.12. Simultaneous topographic and surface potential images of the MBE layers.	202
7.13. A line profile taken from the surface potential image. (a) The location of the line in the KFM image; (b) Comparing the measured data with the calculated data.	204
8.1. Classification of various SFM modes.	208

ABSTRACT

The Atomic Force Microscope (AFM) is an important instrument measuring surface topography and related phenomena; and can study nanometer-scale surface interactions. Surface interactions in ambient air are complicated by surface contamination layers, which do not occur in vacuum or liquid environments. This thesis studies nanometer scale surface interactions, in ambient air, using AFM's high force sensing capability. Several experimental methods were developed and new insights into surface interactions at nanometer scale were obtained. Substantial improvement was made on the lateral resolution of AFM operation in air.

To position the force sensing tip over a specific nanometer scale area, a novel instrument combining AFM and Scanning Electron Microscopy (SEM) was designed, built and commissioned. The system is capable of analyzing AFM tip conditions, in order to study the effects of tip/surface contact. An essentially new method, which monitors the dynamic sensor signal and its fluctuation while changing the tip-sample gap, was developed for vibrating cantilever studies. Sometimes, an electrostatic force occurs in surface contamination, which can be measured with scanning Kelvin-probe force microscopy (KFM); this made it possible to develop a technique for probing surface contamination electrical properties.

A capillary force is associated with the contamination layer. Both capillary force magnitude and layer thickness were measured by fitting the approach curve with the capillary force theoretical model. Studying capillary force with cantilevers of differing spring constants, we demonstrated that capillary force can be balanced by a cantilever having a sufficiently large spring constant. With KFM, the contamination layer was found to contain a charge distribution that changes with time. A model is proposed, showing that the surface contamination layer contains a molecular layer bonded tightly to the sample surface. With KFM, dopant concentration was measured on an MBE-grown semiinsulating sample cross-section, and electrical potential scan edge effect was observed. Systematically studying tip-sample contact, two types of contact processes were identified: jump-to-contact and ramp-to-contact, and the conditions under which they occur. A new spatial region (near-contact region), minimizing tip-sample gap without tip-sample contact, was discovered. Operating in the near-contact region is the optimal operating mode of a vibrating cantilever AFM.

ACRONYMS

AFM	atomic force microscope/microscopy
EFM	electrical force microscopy
FIB	focused ion beam
JTC	jump-to-contact
KFM	Kelvin-probe force microscope/microscopy
MBE	molecular beam epitaxy
MFM	magnetic force microscopy
NSOM	near-field scanning optical microscope/microscopy
PPM	proximal probe microscope/microscopy
PZT	lead-zirconium-titanate
RHEED	reflection high energy electron diffraction
RTC	ramp-to-contact
SEM	scanning electron microscope/microscopy
SFM	scanning force microscope/microscopy
SPM	scanning probe microscope/microscopy
STM	scanning tunneling microscope/microscopy
UHV	ultra high vacuum
VCM	vibrating cantilever mode
VLS	vapor-liquid-solid
VSM	vibrating sample mode

CHAPTER 1

INTRODUCTION

Atomic Force Microscopy (AFM) is a new form of microscopy for imaging surface topography in the nanometer scale. The method was first introduced by IBM and Stanford scientists in 1986,¹ where they demonstrated the proof-of-concept and the outline of the various operation modes. Considerable effort was made in the development and application of this kind of instrument. Perhaps the first method commonly used was to drag the tip across the surface and measure the deflection of the tip mounted on the end of a cantilever.² Although significant success was achieved with this method,^{3,4} it can result in significant tip and/or sample damage.⁵ To obtain non-destructive measurements, tip-sample contact needed to be minimized, which was accomplished by using vibrating cantilever methods.⁶

To understand the mechanism of the microscopy techniques, one should study the tip-sample interaction, which is influenced by the environment. For air operation, the interaction is complicated by the existence of surface contamination. The commonly used technique to study tip-sample interaction is to measure the dependence of the cantilever force on the tip-sample gap.⁷ As frequently observed in loading curves measured in air, the tip can be pulled into contact with the sample by the sample's surface and its contamination. This jump-to-contact behavior results in tip and/or sample damage.

Two major operating modes were developed for the vibrating cantilever AFM. These old modes presented a number of problems when operating in ambient air. In the traditional non-contact mode,⁶ the existence of surface contamination layer results in a large tip-sample gap, which

limits AFM's lateral resolution. In microscopy, lateral resolution generally means the smallest feature that can be resolved by a microscope. When the tip is brought into the contamination layer, the capillary force between the tip and the sample can capture the tip to the sample surface, which stops the vibration of the cantilever. In the "tapping" mode⁸ proposed later, the cantilever is set to vibrate at much larger amplitudes (> 20 nm), which results in periodic contact between the tip and the sample. Such physical contact, although it can be very light, damages the tip and/or sample when operating in air, and limits the lateral resolution.

The objective of this thesis is to understand the physics of nanometer scale surface interaction with the presence of surface contamination layers, and to understand the working mechanism of vibrating cantilever mode AFM to optimize imaging resolution. The results of this thesis research can be summarized in five areas. The first is the development of new experimental apparatus and methods. The second is the understanding of the surface contamination layers in ambient air. The third is the understanding of the capillary force due to the surface contamination at nanometer scale. The fourth is the study of surface electrical potential at nanometer scale. The fifth is the understanding of surface contact at nanometer scale in ambient air. The observation and discoveries on the physics of nanometer scale tip-sample interaction in ambient air leads to new insights on the working mechanism of vibrating cantilever AFM, and the development of a new operating mode for the vibrating cantilever AFM in air.

To study the nanometer scale surface interaction, we developed a number of new experimental techniques during the course of this thesis work. To precisely position the force sensing tip over a specific nanometer scale area, we built the first instrument that combines AFM and scanning electron microscopy (SEM). This system is also capable of analyzing the conditions of the force-sensing tip for studying the effects of tip-surface interactions. To permit proper comparison between conventional loading curve measurements and theoretical models of surface interactions, an analysis method for removing the effect of cantilever deflection for the loading curves was used. A

novel method was demonstrated for studying the interaction between a vibrating tip and a surface, in which the dynamic sensor signal and its fluctuations are monitored while changing the gap between the tip and the surface. To study the surface electrostatic interaction, a scanning Kelvin-probe force microscopy (KFM) system was built as an addition to the vibrating cantilever AFM. We developed a new method that can detect the surface contamination layer by monitoring the time dependence of the KFM signal.

It is generally acknowledged that a "contamination" layer exists on the surface of a sample in ambient air.⁹ However, the nature of this contamination layer is not well understood. In this thesis, the thickness of the contamination layer was measured for the first time by comparing the loading curves measured in air and in vacuum and fitting the approach curve in air with the theoretical model of capillary force. By comparing the loading curves measured in air and under vacuum, we found that the contamination layer is a major factor contributing to the fluctuation of loading curve measurements. With the KFM, we found that the contamination layer contains a space charge distribution that varies with time, which confirms the liquid-like property of the contamination. We proposed a structural model of the surface contamination layer that consists of a molecular layer that is bonded tightly to the sample surface. This model explains our observations of various surface interactions at nanometer scale.

It is generally acknowledged that when a tip and a surface make contact in the presence of contamination layers, a capillary force exists between the tip and the surface.¹⁰ The magnitude of the capillary force between a nanometer sized tip and a surface coated with contamination layers is not well understood. It was believed that an AFM cantilever could not overcome the capillary force and would be captured to the surface when the tip-sample gap is less than a few nanometers. In this thesis, we measure the magnitude of the capillary force by fitting the theoretical model of capillary interaction to the loading curves that we measured. By studying the capillary force with cantilevers of different spring constants, we demonstrate that the capillary force can be balanced by cantilevers having adequately large spring constants.

Using KFM, the time dependence of the electrostatic interaction after a step change of the bias voltage was investigated. The process of redistribution of surface charge was observed. The surface electrical potential on a cross section of an MBE grown semi-insulating sample was measured and fitted with a theoretical model to obtain the dopant concentration. The unique edge-effect phenomenon of electrical potential was observed at the edge of the cross-section of an MBE prepared sample.

It is generally acknowledged that the tip and/or sample may sustain damage when they are brought into contact. However, the physics of nanometer scale surface contact in the presence of surface contamination layers, and the mechanism of surface damage are not well understood. With the combined AFM/SEM system, we found three types of nanometer scale tip damage. We also observed, for the first time, the sample damage due to minimal contact when the sample is scanned with large-amplitude vibrating cantilever AFM in ambient air. Two types of contact processes were identified: jump-to-contact (JTC) and ramp-to-contact (RTC). We established the conditions in which JTC and RTC occur. We then discovered a very narrow spatial region at close proximity to the surfaces, designated as the "near-contact region", where the tip-sample gap is minimized and physical contact between tip and sample does not occur. Maintaining an AFM tip in the near-contact region is critical for obtaining maximum lateral resolution in AFM images. We established the optimal parameters in vibrating cantilever modes for making high resolution AFM topographic images.

The suggestion of completing this Ph.D. thesis research at TopoMetrix was initiated by Dr. P. West in early 1992 and approved by the Graduate Committee in February 1992. The design of the first version of the combined PPM/SEM instrument began on January 1993. The design of the final version was completed on August of 1993 and was granted a United States Patent on October 1995.¹¹ Most of the experimental work was done in 1994 and the first half of 1995. Some of the results were presented at the 1995 APS March Meeting, and a paper was submitted to *Scanning*

for publication on September of 1995 and published in August 1996.¹² The writing of this thesis began in the late summer of 1995 and was severely interrupted by the decease of my daughter, Rebecca, at the end of 1995. The review of the thesis by the advisors began on August of 1996, and the defense was on March 7, 1996. In addition to the academic results, this thesis research also generates three major results of interest to the PPM industry. It resulted in the world's first and still the only commercial SPM instrument combined with a SEM, the first commercial scanning electrical potential microscopy, and a new working mode, near-contact mode, for vibrating cantilever AFM.

Most of the work in this thesis was done by the author alone, including the design and construction of the instrument, planning and set-up of the experiments, processing and analysis of data, and development of theoretical models and analysis. During the course of this thesis work, direct assistance was given by a number of people. Dr. Paul West initiated the original concept of a combined AFM/SEM instrument and provided the name, Near Contact, to our new AFM operating mode. Mr. Marc Schuman designed the electronics for the double-feedback-loop system. Mr. E. Hazaki of Hitachi Scientific Instrument provided the first evidence of the laser-heating problem in the combined PPM/SEM instrument, which was later corrected by the author's modification of the design. Fabrication of the KFM standard sample was arranged by Dr. P. Chiang. The MBE-grown multilayer GaAs sample was specially grown by Dr. H.-S. Wu for this thesis.

The writing of this thesis has been a significant learning process in my career. I learned how to communicate professional knowledge with people who come from different backgrounds, and acquired the skills associated with drawing conclusions from vast amounts of data, ideas, and conjectures.

Since PPM is a relatively new area of scientific study, a large number of new concepts may be encountered by the reader. The layout of this thesis is presented in such a way as to help the reader understand the body of the thesis work. Chapter 2, Historical Review, presents the history of pre-

vious developments in PPM related areas. It also introduces a number of important concepts that will be used in discussion of the following chapters. Chapter 3, Theoretical Analysis, presents the theoretical analysis of various subjects related to this thesis work. It focuses on the discussion of nanometer scale tip-sample interaction. Chapter 4, Experimental Apparatus, describes the instruments and experimental methods used in this thesis work. Chapter 5, Studies of AFM Loading Curves, discusses the experiments and results on the study of the nanometer surface interaction with a DC method (loading curve measurement). Chapter 6, Studies of Vibrating Cantilever Mode (VCM), discusses the experiments and results on the study of the nanometer surface interaction with an AC method (vibrating cantilever). It also presents a theoretical model that explains the nanometer scale tip-sample interaction in air and the working mechanism of VCM, and the new operation mode that maximizes lateral resolution for AFM in air. Chapter 7, Imaging Surface Electrical Potential, deals with the experiments with KFM. Chapter 8, Conclusion, presents the summary of the observations and discoveries of the physics of nanometer scale surface interaction in air and the working mechanism of AFM, and the development of experimental techniques that resulted from this thesis research.

CHAPTER 2

HISTORICAL REVIEW

Introduction

Using a material probe to detect a surface by touching it to the specimen is a natural concept. For instruments that measure surface topography, a material stylus maintained at close proximity to the sample surface is used to perform the measurement. For many years, surface profilers with a stylus tip have been used to measure the surface profile.¹³ The topografiner,¹⁴ invented in 1972, was the first surface profiler that achieved sub-micrometer lateral resolution. It was the first instrument using piezoelectric ceramics to scan the tip across the surface, and it achieved one nanometer vertical resolution with a feedback system. About ten years later, a breakthrough was made by G. Binnig and H. Rohr¹⁵. They demonstrated that the atomic structure on surfaces could be imaged using quantum tunneling between a sharp metal tip and the sample. This work opened the door to using material probes as a microscopy tool. They called their new instrument the Scanning Tunneling Microscope (STM).

Although it is powerful enough to image surface atoms, the STM has a significant shortcoming. Since the electron tunneling effect is used in an STM to detect the sample surface, it requires the sample to have some conductivity. However, a large portion of the material world is non-conducting, which substantially limits the application of the STM. To image the topography of non-conducting materials, a tip-sample interaction independent of sample conductivity must be used. The interaction forces that exist between a tip and any solid sample are substantially large when the tip is brought to within a few nanometers of the sample surface. These forces exist inde-

pendently of the electrical conductivity of the sample. Therefore, a force sensor that detects these forces can be used to sense the proximity of any sample surface. In 1985, a high-sensitivity force sensor was developed based on an STM. With this force-sensing technique, the first atomic force microscope (AFM) was invented.¹

The STM, AFM, and all the related technologies that use a material probe to perform microscopic imaging at close proximity of a sample surface have been grouped into the term scanning probe microscopy (SPM). Recently, a new term, Proximal Probe Microscopy¹⁶ (PPM), has been used. This new term is more appropriate in distinguishing solid material probes from particle probes, such as electron probes and ion probes. The word "proximal" emphasizes that our scanning probes are operating in the near-field¹⁷ condition.

Each PPM involves a physical property that strongly depends on the spacing between the tip and the sample, and a sensing system built to detect this physical property. The tip-sample gap is controlled by a piezoelectric actuator, and this spacing can be maintained by feedback electronics that receives the input signal from the sensing system and controls the piezoelectric actuator. Because this piezoelectric actuator moves the probe perpendicular to the sample, it is commonly called the *Z piezo*. When the tip-sample gap is maintained constant by the feedback electronics, we say the PPM system is *in topographic feedback* (or *in feedback* as the abbreviation), and call the system a *topographic feedback loop*. While the tip-sample gap is maintained constant, that is, when the PPM is in feedback, the surface topography can be obtained from the displacement of the *Z piezo*, which is a function of the voltage applied to the piezo. A piezoelectric *XY scanner* (also called *XY piezo*) is another important component of PPM, which scans the tip across the sample surface while the *Z piezo* voltage is being recorded. The spatial distribution of the recorded *Z piezo* voltage can be used to generate an image representing the topography of the sample being measured, which is also called *to image* the surface topography. The smallest step size of a piezoelectric scanner can be less than one angstrom, which helps the PPM to image atomic structures.

The operation of PPM involves two major steps (Figure 2.1). The first is tip-approach, which

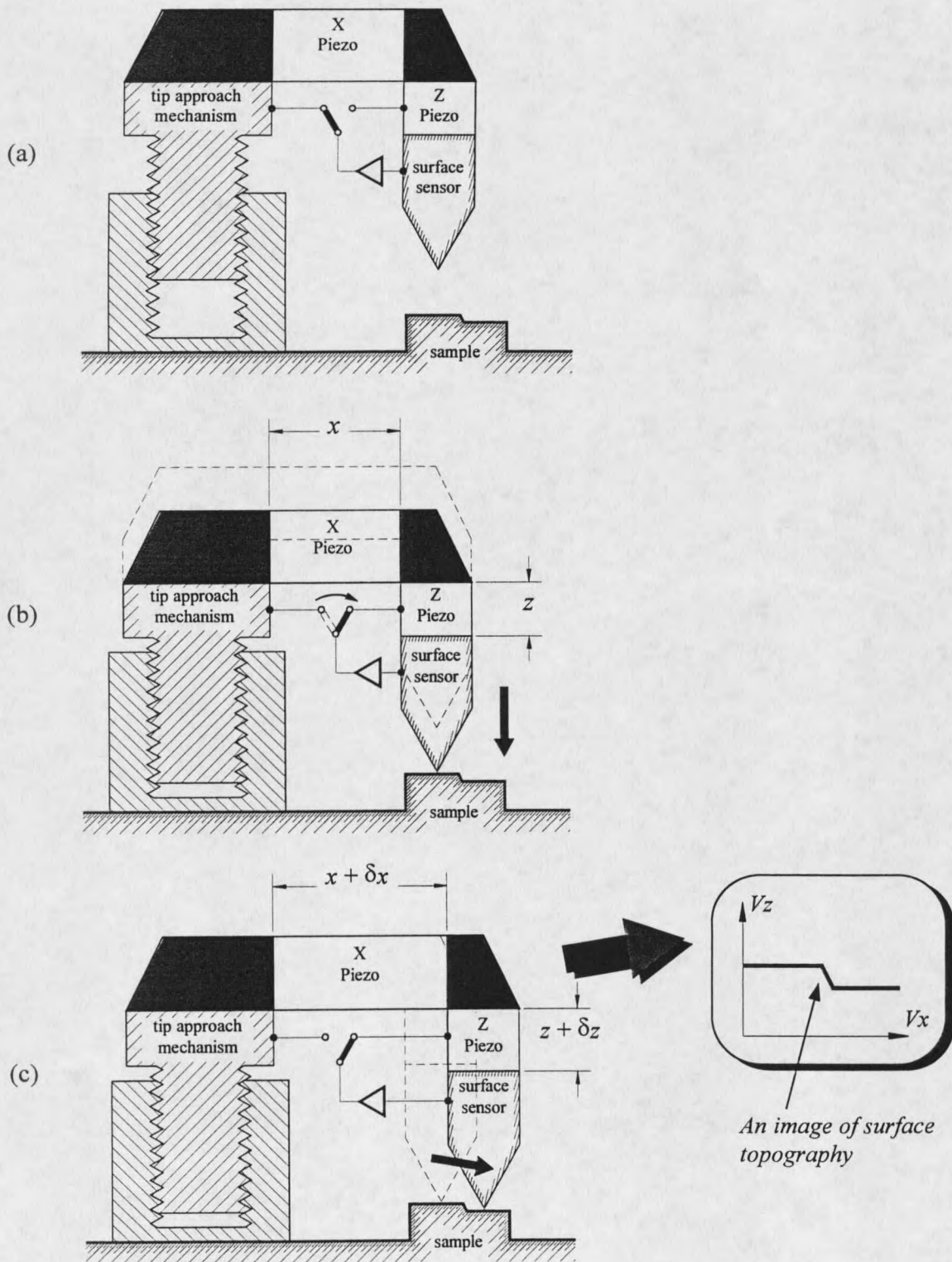


Figure 2.1. The operation of a PPM. (a) Initial set-up; (b) The tip approach process; (c) The scanning process.

is a process that brings the PPM probe from a macroscopic tip-sample gap to where the tip-sample gap is on the order of a few nanometers or less. Compared to other scanning microscopies, this step is unique for proximal probe microscopy. The second step is to scan the probe across the sample surface to acquire an image while the tip is maintained in the proximity of the sample surface by the topographic feedback loop. The topographic image is generated by plotting the Z piezo voltage versus the XY piezo voltages.¹⁸ Since a topographic image of PPM is created by the voltages applied to the piezo scanners, the image is generally independent of the physical property used to sense the sample surface.

By the use of additional sensors or additional sensing techniques, other surface physical properties, such as electrical potential, can also be measured simultaneously with topography. While the XY piezo scans the tip across the sample surface, these other physical properties can be recorded along with the topography. The spatial distribution of a recorded signal output of an additional sensor can be used to generate an image representing the physical property being measured, which is also called *to image* this physical property.

PPM has a number of advantages over other microscopy techniques. Its resolution is higher than traditional optical microscopy and the SEM, permitting it to image local surface topography and electrical structure at the atomic scale. Many other physical and chemical properties can also be imaged in sub-micrometer scale resolution, and experiments on the nanometer scale is possible. All PPMs can be operated in air, vacuum, or other environments, which greatly increase the application area of the PPM.

The topographic images that PPM generates are three-dimensional. On very flat samples (roughness < 10 nm), PPM images have much higher topography contrast than Scanning Electron Microscopy (SEM). Because the contrast of a SEM image is created by the difference in the secondary emission of surface material or change of slope on surface topography, a flat surface of uniform material results in very low contrast for SEM. However, PPM records surface topography

with the position of the piezoelectric actuator that controls the feedback. The image contrast in surface topography is limited by the voltage noise on the piezoelectric actuator and environmental vibration, which can usually be made small enough to allow the system to detect topographic variation of less than one nanometer. For SEM, non-conductive samples must be coated with conductive material to obtain high-resolution images. For AFM imaging, since the image mechanism does not require any conductivity of the sample, the conductive coating is not necessary.

The major limitations of PPM are caused by the limited Z piezo range (usually smaller than 10 μm) and the tip geometry. PPM imaging is restricted to relatively flat samples. The fluctuation of surface topography must be smaller than the range of Z piezo. However, SEM does not have such a restriction, enabling imaging of porous or very rough sample.

Because of the prospect of imaging atoms, the novel imaging mechanisms, capability of exploring the nano world, along with modern computer technologies, and the quest by researchers from various fields to see ever smaller objects, PPM quickly became one of the most important microscopy techniques for academic research and industrial applications.

Nanometer Scale Force Sensing Techniques

To perform high-resolution imaging, the tip must be brought very close to the surface, usually 10 nm or less. A sensing technique that detects the change in tip-sample gap is necessary to bring the tip into proper working position. Since interaction forces between the tip and the sample strongly depend on the tip-sample gap, various surface-force-sensing techniques were developed for controlling the tip-sample gap. A PPM equipped with one of the surface-force sensing techniques is called a Scanning Force Microscope (SFM). Depending on the direction of the force to be detected (vertical or lateral), the microscopic force sensing techniques can be classified into two types: *normal force sensor* and *shear force sensor*.

Most of the microscopic force sensing techniques used in the SFM are normal force sensors which include a microscopic cantilever that converts the variation of the tip-sample interaction

force into the cantilever movement, and a displacement-sensing device that detects the movement of the cantilever (see Figure 2.2). Historically, this type of microscope has been called the Atomic Force Microscope (AFM).^{1,19}

The shear-force sensing technique uses a rigid tip (like in the STM) which is positioned perpendicular to the sample surface, and is set to vibrate parallel to the surface (see Figure 2.3). When the gap between the tip and the sample is small enough, the tip-sample interaction will be strong enough to change the resonance characteristics of the tip, which can be detected. The detailed mechanism of the change of the resonance characteristics will be explained later in Chapter Three. This technique has been used for the Magnetic Force Microscopy (MFM), and is especially useful for the optical fiber tips used in the Near-field Scanning Optical Microscopy (NSOM).

Cantilever-Based Force Sensors

The cantilever-based force sensor is the sensor used in AFM. Various techniques of detecting microscopic spatial displacement have been developed for the cantilever-based force sensor. Most of these sensing techniques can detect a displacement of the cantilever on the order of one angstrom or less. Since tip-sample interaction forces are usually of the order of a nano-newton, a microscopic cantilever with spring constant of less than 1 newton/meter is a suitable device to convert such microscopic forces into microscopic movement. The processes for large-scale production of microscopic cantilevers by photolithography techniques have been developed.²

Figure 2.2 shows the basic components of a cantilever-based force sensor. It consists of a cantilever, a material stylus, and a displacement sensor. The probe generally has an aspect ratio (which is the ratio of the probe height to the maximum probe width, see Figure 2.2) of greater than one. In most cases, the displacement sensor is external and is located behind the cantilever. When the electromechanical effect (such as piezoelectricity and piezoresistivity) of the material of cantilever is used to detect the cantilever displacement, the cantilever itself can be an internal displacement sensor.

